# Bimodality in a Monostable Climate–Ecosystem: The Role of Climate Variability and Soil Moisture Memory*

ZHENGYU LIU

*Center for Climatic Research, and Department of Atmospheric and Oceanic Sciences,
University of Wisconsin—Madison, Madison, Wisconsin*

(Manuscript received 6 April 2009, in final form 15 October 2009)

## ABSTRACT

The probabilistic modal response of vegetation to stochastic precipitation variability is studied in a conceptual climate–ecosystem model. It is found that vegetation can exhibit bimodality in a monostable climate–ecosystem under strong rainfall variability and with soil moisture memory comparable with that of the vegetation. The bimodality of vegetation is generated by a convolution of a nonlinear vegetation response and a colored stochastic noise. The nonlinear vegetation response is such that vegetation becomes insensitive to precipitation variability near either end state (green or desert), providing the potential for two preferred modes. The long memory of soil moisture allows the vegetation to respond to a slow stochastic forcing such that the vegetation tends to grow toward its equilibrium states. The implication of the noise-induced bimodality to abrupt changes in the climate–ecosystem is also discussed.

## 1. Introduction

Classical theories on the abrupt changes of the climate–ecosystem have focused on the feedback mechanism and the equilibrium response. With strong positive feedbacks, the coupled system can exhibit multiple equilibria and strong hysteresis behavior (Claussen 1998; Brovkin et al. 1998), providing a fundamental mechanism for abrupt changes (Claussen et al. 1999). However, there is significant climate variability, notably in precipitation and in arid regions where precipitation variability is significant relative to its climatological mean. The role of strong climate variability on the abrupt change in a coupled climate–ecosystem remains poorly understood. In general, a simple random noise tends to act as a "mixing" on the coupled state (e.g., Stommel and Young 1993; Rodriguez-Iturbe et al. 1991) and therefore tends to suppress abrupt changes (Liu et al. 2006, hereafter LIU). However, a more general climate "noise" forcing may exert a much more complex impact that can be opposite to the mixing effect. Indeed, a climate noise can induce new preferable states, or prob-

abilistic modes, through its interaction with the dynamic system as a multiplicative noise (Rodriguez-Iturbe et al. 1991) or through its increased memory as a colored noise (Timmermann and Lohmann 2000; Monahan et al. 2002). These noise-induced probabilistic modes provide another mechanism for abrupt changes in the climate–ecosystem.

As a pilot study here, we will study the probabilistic modes in a conceptual climate–ecosystem, with the focus on the generation of new probabilistic modes in a monostable system. This study is motivated by our recent attempt to understand the collapse of the Africa monsoon–ecosystem in the mid-Holocene in the observation (deMenocal et al. 2000) and in a complex earth system model (LIU). LIU proposed that, even in a monostable climate–ecosystem, the ecosystem can collapse abruptly when the coupled system is forced by a strong stochastic forcing in the presence of a long soil moisture memory. This type of abrupt change in a monostable system, known as the stable collapse, is in contrast to the classical mechanism of abrupt change in a bistable climate–ecosystem (Claussen et al. 1999) and other climate systems (e.g., Cessi 1994; Timmermann and Lohmann 2000). However, LIU only presented a few examples of the abrupt changes in a monostable system. It remains unclear what mechanism is responsible for this abrupt change and how the abrupt change depends on model parameters. Here, we will further study the

---

\* Center for Climatic Research Contribution Number 985.

*Corresponding author address:* Z. Liu, CCR, 1225 W. Dayton St., Madison, WI 53706.
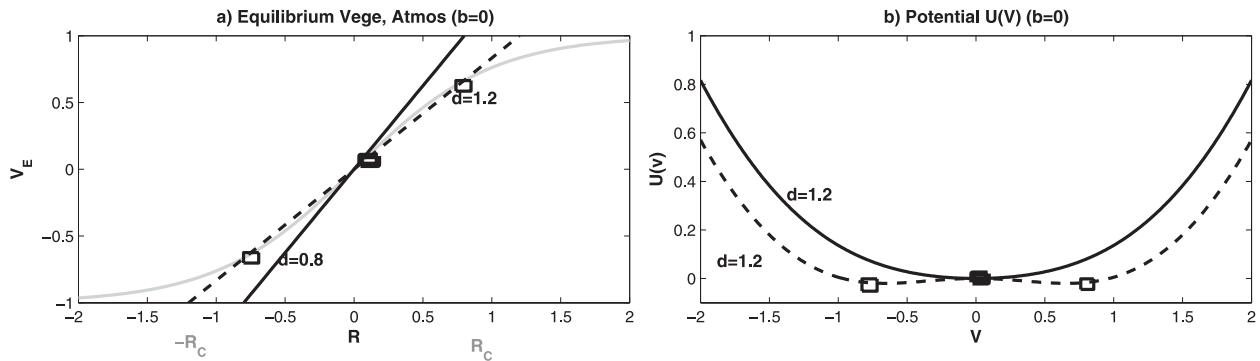E-mail: zliu3@wisc.edu

FIG. 1. Equilibrium states for $b = 0$. (a) Equilibrium vegetation response function (gray), equilibrium atmosphere for the weak feedback case ($d = 0.8$, solid), and strong feedback case ($d = 1.2$, dash). (b) The potential function for the monostable ($d = 0.8$, solid) and bistable ($d = 1.2$, dash) system. The three squares mark the equilibrium solutions, and $R_C$ marks the approximate range of climatological rainfall by which vegetation changes between green and desert states at quasi equilibrium.

mechanism of abrupt change in the monostable climate–ecosystem systematically in terms of its probabilistic states. It is shown that the random precipitation, the nonlinear vegetation response, and the slow soil moisture memory together generate a bimodality in the monostable system similar to that in a bistable system. This generation of bimodality provides a new mechanism for the abrupt transition in a climate–ecosystem.

In the following, we will first introduce the coupled climate–ecosystem model in section 2. We will then examine the development of the bimodality, first in the fully coupled system in section 3 and then in reduced systems in section 4. A summary and implications will be given in section 5.

## 2. The coupled climate–vegetation–soil model

We use a conceptual climate–vegetation system similar to those of Brovkin et al. (1998) and LIU. With proper nondimensionalization, the nondimensional vegetation–climate system can be written in vegetation cover $V$ ($-1 < V < 1$) and annual rainfall $R$ as

$$\frac{dV}{dt} = V_E(R) - V,  \tag{1}$$

where $V_E(R) = \tanh R$ and

$$R = R_E(V) + N(t),  \tag{2}$$

where $R_E(V) = b + dV$.

The vegetation cover $V$ is relaxed toward its equilibrium state $V_E$ in a unit time; $V_E$ is determined by the total rainfall $R$ through the nonlinear vegetation response function $\tanh R$. The $V_E$ approaches the green state $V \sim 1$ for rainfall exceeding $\sim R_C$, and approaches the desert state $V \sim -1$ for rainfall below $\sim -R_C$ (Fig. 1a), with $2R_C \sim 2$ being a measure of the rainfall climatology that

enables the equilibrium vegetation to switch between the green and desert states. Rainfall $R$ consists of an equilibrium response $R_E$ and a stochastic variability $N(t)$; $R_E$ consists of a background rainfall $b$ and a feedback parameter $d$, with $d > 0$ for positive vegetation feedback on rainfall; $N(t)$ represents the rainfall variability associated with internal atmospheric instability. For simplicity, here the total rainfall is no longer lower bounded.

A single equation for the coupled system can be derived by inserting Eq. (2) into Eq. (1) as

$$\frac{dV}{dt} = \tanh(dV + b + N(t)) - V$$

or

$$\frac{dV}{dt} = -U'(V) + S(V, N).  \tag{3}$$

Here $U$ is the equilibrium potential

$$U(V) = -\int_0^V (\tanh[dv + b] - v)\, dv$$
$$= \frac{V^2}{2} - \frac{\ln[\cosh(dV + b)]}{d},  \tag{4}$$

and $S$ is the stochastic forcing

$$S(V, N) \equiv \tanh(dV + b + N) - \tanh(dV + b)  \tag{5}$$

that diminishes with $N$ as $S(V, N) \xrightarrow{N \to 0} 0$.

In the absence of stochastic forcing, the coupled system (3) is monostable for weak vegetation feedback $d \le 1$ and bistable for strong positive vegetation feedback $d > 1$. The case of a small or zero $b$ gives the potential of the classical two-well potentials symmetrically around $x = 0$. Figure 1 shows two examples for $b = 0$, one weak feedback

($d = 0.8$) and the other strong feedback ($d = 1.2$), with the equilibrium atmospheric models shown in Fig. 1a (as straight lines) and their potentials in Fig. 1b. The system $d = 0.8$ has a single stable equilibrium at the medium vegetation state ($V = 0$); the system $d = 1.2$ has two stable equilibria (a green state $V \approx 0.8$ and a desert state $V \approx -0.8$) and an unstable equilibrium ($V = 0$).

For the application to the coupled climate–ecosystem, LIU suggested a further improvement to include the effect of soil moisture memory. Conceptually, the rainfall $R$ that forces vegetation in Eq. (2) should be thought as the soil moisture because vegetation is determined directly by soil moisture rather than rainfall. This difference between soil moisture and precipitation may not be important for the equilibrium response but is critical for the variability response and in turn new probabilistic modes, as inferred from LIU. Intuitively, soil moisture has a memory comparable with that of the vegetation such that the direct stochastic forcing on vegetation should be represented by a red noise in soil moisture, instead of a white noise in rainfall. In LIU, the effect of soil moisture memory is represented crudely as a running mean on white noise precipitation variability. Here, the effect of soil moisture memory will be represented more formally by treating $N$ as a red noise process. With a variance of $M^2 = \sigma^2/(2\tau)$ and a persistence time representative of the soil moisture memory of $\tau$, the $N$ can be obtained from a conceptual "soil moisture" equation forced by a random rainfall variability of a variance $\sigma^2$ as

$$\frac{dN}{dt} = \frac{-N}{\tau} + \frac{\sigma \varsigma(t)}{\tau}, \quad (6)$$

where $\varsigma(t)$ is a white noise process with a unit variance. It is important to point out that in Eq. (6) $N$ represents an idealized one-way forcing of soil moisture on vegetation. In more realistic scenarios, soil moisture dynamics is much more complicated because it interacts with vegetation and surface climate. In the absence of the direct vegetation–climate interaction, previous studies show that vegetation–soil moisture interaction (e.g., Zeng et al. 2005) or soil moisture–climate interaction (e.g., Rodriguez-Iturbe et al. 1991) alone may lead to strongly nonlinear behavior and multiple preferred states in the coupled system. Since our purpose here is to highlight the new effect due to vegetation–climate feedback, we will only use the idealized "soil moisture" equation (6), which has feedbacks from neither vegetation nor surface climate. Keeping in mind this idealized nature of our "soil moisture" variability $N$, here we will simply call $\sigma$ and $M$ the intensities of rainfall variability and "soil moisture" variability, respectively, and $R$ the total "soil moisture". Equations (3) and (6) form our coupled climate–vegetation–soil moisture system.

## 3. Bimodality in the full model

The climate–ecosystem (3) and (6) is nontrivial as a nonlinear stochastic differential equation because the stochastic noise is nonlinear and is colored. There is no general analytical approach for the probabilistic density function (PDF) of such a system. Therefore, the PDF will be obtained numerically using a forward Euler discretization (Kloeden and Platen 1992) as

$$V_k = V_{k-1} + \Delta t (-U'(V_{k-1}) + S(V_{k-1}, N_{k-1}))N_k$$
$$= N_{k-1} - \frac{\Delta t}{\tau} N_{k-1} + \sqrt{\Delta t} \frac{\sigma}{\tau} W_{k-1}. \quad (7)$$

Here $\Delta t$ is the time step; subscript $k$ is the value at time $k\Delta t$; $\{W_k\}$ is a sequence of Gaussian random variable with a zero mean and unit variance. Each PDF is obtained from an integration of 100 000 time units with a time step $\Delta t = 0.3$. Our results are robust with respect to the time step and integration length. Unless otherwise specified, we will discuss the system of a medium background rainfall of $b = 0$, such that the PDF should be symmetric about $V = 0$.

The stationary PDF for the monostable system $d = 0.8$ is shown for 3 cases with extended soil memories of $\tau = 0.3$, 1, and 2 [Figs. 2a(1)–(3)], each case forced by 4 successively stronger rainfall variability $\sigma = 0.2$, 0.5, 1, and 2. Since this system has a single equilibrium at $V = 0$ (Figs. 1a,b), one expects a unimodal PDF of $V$ with the peak at $V = 0$. This is true, as seen for the weak forcing of $\sigma = 0.2$, regardless of the soil memory. As the forcing increases to $\sigma = 0.5$, the peak of the PDF is broadened by the "mixing" effect of the noise. As the forcing further increases to $\sigma = 1$, the PDF changes dramatically with the emergence of a bimodal PDF when soil memories are comparable or longer than that of the vegetation, as seen for $\tau = 1$ and 2 [Figs. 2a(2),(3)].

As a quantification of bimodality, we define an index of double-peak intensity (DPI) for a symmetric PDF $p(V)$ as

$$\text{DPI} \equiv \frac{\max(p(V)|_{V>0}) + \max(p(V)|_{V<0})}{2p(0)} - 1. \quad (8)$$

The DPI is zero if the PDF has a single peak at $V = 0$ but becomes positive when bimodality emerges. The larger the DPI, the more prominent the double peak. In the monostable system in Figs. 2a(2) and 2a(3), the bimodality PDFs for $\sigma = 2$ have DPI $= 0.25$ and 1, respectively.

The DPI is calculated systematically in Fig. 3a for the monostable system $d = 0.8$ as a function of soil memory ($0.3 \leq \tau \leq 4$) and forcing magnitude ($0.2 \leq \sigma \leq 3$). As discussed, Fig. 2a, DPI is small for either weak forcing or short soil memory. For example, DPI $< 0.5$ for $\sigma \leq 1$
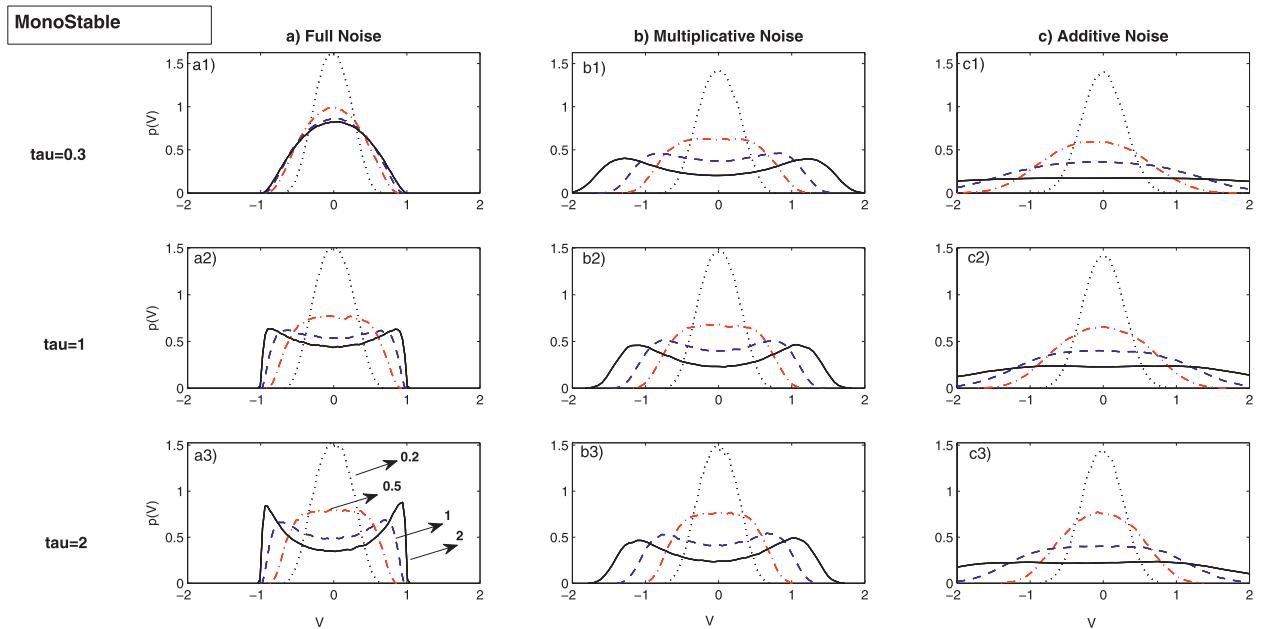
FIG. 2. Stationary PDFs for the monostable system $d = 0.8$. (a) Full model solution for soil memories (top) $\tau = 0.3$, (middle) $\tau = 1$, and (bottom) $\tau = 2$. (b) Similar to (a) but for the reduced model of multiplicative noise; (c) similar to (a) but for the reduced model of additive noise. In each panel, four rainfall magnitudes are used: $\sigma = 0.2$ (dot), $\sigma = 0.5$ (dash–dot), $\sigma = 1$ (dash), and $\sigma = 2$ (solid), as marked in [a(3)].

or $\tau \le 1$. With a further increase in both the forcing and soil memory, DPI becomes significantly positive, indicating a distinct bimodality. For large forcing and long memory, the DPI increases monotonically with the forcing amplitude but appears to saturate at a soil memory $\tau_S(\sigma)$ that increases with the forcing magnitude. For the system of $d = 0.8$ here, the saturation level increases with the forcing roughly as $\tau_S(\sigma) \sim \sigma$.

It is interesting that the bimodal PDF requires a strong precipitation variability $\sigma \ge 1$, but not necessarily a large soil moisture variability $M = \sigma/\sqrt{2\tau}$. Indeed, the strong dependence of bimodality on $\sigma$, rather than $M$, can be seen clearly in Fig. 3a, where the heavy dash line represents the boundary of $M = 1$: significant bimodality develops for $M < 1$ (lower part) as long as the soil memory is sufficiently long. It is nevertheless interesting in Fig. 3a that the critical soil moisture variability $M \sim R_C$ coincides approximately with the saturation level $\tau_S(\sigma) \sim \sigma$.[1] In the equilibrium vegetation response, the transition between a green and desert state is possible

only if the total soil moisture $R$ varies with a range comparable or larger than $R_C \sim 1$ (see Fig. 1a). This is not the case for the generation of bimodality by stochastic forcing. For example, for the case of a long memory $\tau = 2$ [Fig. 2a(3)], significant bimodal PDF emerges for $M$ as low as 0.25 (at $\sigma \sim 1$).

The bimodality in a monostable system resembles somewhat that in a bistable system, for example, with $d = 1.2$ (Fig. 4a). This bistable system has a classical double-well potential (Fig. 1b) and therefore is expected to exhibit a bimodality. This is confirmed in Figs. 4a(1)–(3) under a weak forcing $\sigma = 0.2$, where a significant bimodality exists regardless of the soil memory. As the forcing intensifies, however, bimodality is suppressed by the mixing associated with stochastic variability. With a short memory $\tau = 0.3$ [Fig. 4a(1)], interestingly, bimodality is suppressed for strong forcings. For a given forcing magnitude, however, as the soil memory increases, bimodality recovers [Figs. 4a(2),(3)]. Therefore, for strong forcing $\sigma \sim O(1)$ and slow memory of $\tau \sim O(1)$, the monostable [Figs. 2a(2),(3)] and bistable [Figs. 4a(2),(3)] systems both exhibit a similar bimodality. Unlike the monostable system when the bimodality saturates with soil memory, the bimodality intensifies with the soil memory in the bistable system. This is seen clearly in the DPI in Fig. 3b: in the limit of large forcing and long memory, DPI increases monotonically with both the forcing and memory. Therefore, DPI is usually larger in the bistable system than in the monostable system for strong forcing, as expected.

---

[1] Formally, $\sigma$ may be treated as the magnitude of equilibrium soil moisture response of $N$, as seen in the soil moisture equation (6) at equilibrium under a long-term rainfall forcing of constant $\varsigma(t) \equiv 1$. Therefore, it appears that bimodality in Fig. 3a emerges when the rainfall variability is sufficiently strong such that its equilibrium soil moisture response of $N$ becomes comparable with $R_C = 1$, and the soil memory becomes comparable or longer than the vegetation memory $\tau > 1$.
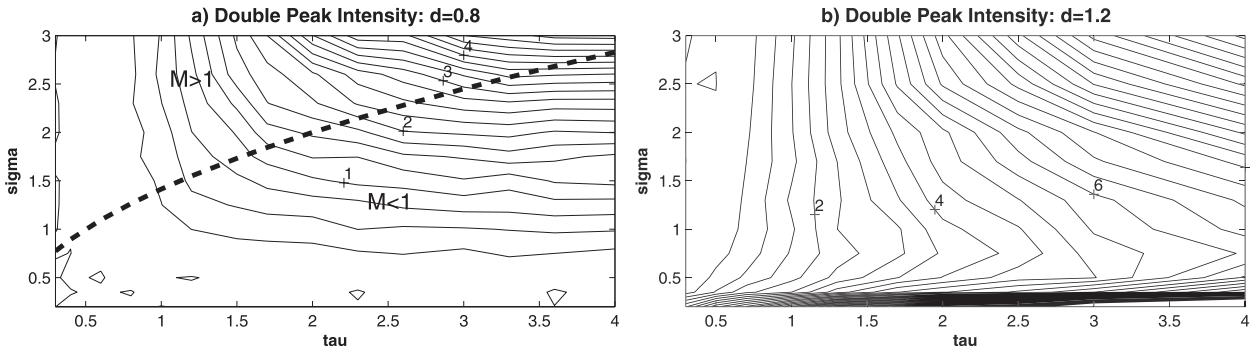
FIG. 3. Double-peak intensity as a function of soil memory $\tau$ and rainfall intensity $\sigma$ for the systems of (a) monostable $d = 0.8$ and (b) bistable $d = 1.2$. The heavy dash line in (a) marks the intensity of soil moisture variability $M = 1$. Contour interval is 0.25 in (a) and 0.5 in (b).

## 4. Mechanism for bimodality

The bimodality in the monostable climate–ecosystem can be contributed in principle by several factors. Soil memory could contribute to the bimodality because a colored noise may shift or induce new modes in a nonlinear system (Hänggi et al. 1990; Timmermann and Lohmann 2000; Monahan et al. 2002). In the meantime, the noise forcing is convoluted nonlinearly with the vegetation system through the vegetation function tanh$R$ and may also change the modality. To better understand the bimodality, especially the roles of the colored noise versus nonlinear noise forcing, we will simplify the full model (3) and (6).

For a small noise, the vegetation–climate model (3) can be approximated as an equation of multiplicative noise:

$$\frac{dV}{dt} = -U'(V) + B(V)N(t), \qquad (9a)$$

where the noise term $S(V, N)$ is approximated by its Taylor expansion with

$$B(V) = \frac{\partial}{\partial N} S(V, N)\big|_{N=0} = \frac{d}{dy} \tanh y \big|_{y=dV+b}$$

$$= \frac{1}{\text{ch}^2(dV + b)}. \qquad (9b)$$

This equation can be further simplified to an equation of additive noise by fixing $B$ as a constant $B_0$, such as $B(0)$:

$$\frac{dV}{dt} = -U'(V) + B_0 N(t). \qquad (10)$$

Now, the vegetation cover is no longer constrained between $-1$ and 1 because of the linearization of the vegetation response function. Nevertheless, these reduced systems can still shed light on the mechanisms of bimodality.

To isolate the effect of the colored noise, we will further simplify the soil moisture equation (6) in the limit of

a diminishing memory $\tau \to 0$. Now, the stochastic soil moisture forcing $N(t)$ approaches a white noise (variance $M^2$) and the PDF for the reduced model of multiplicative noise (9) is determined by the Fokker–Planck equation (in Stratonovich calculus):

$$\frac{\partial p}{dt} = \frac{\partial}{\partial V}\left\{\left(U' - \frac{B_N \partial_V B_N}{2}\right)p\right\} + \frac{\partial^2}{\partial^2 V}\left\{\frac{B_N^2}{2}p\right\}, \qquad (11)$$

where $B_N(V) = B(V)M$ (Gardiner 1997). The stationary PDF can be derived analytically as

$$p(V) = p_0 \exp(-\Psi(V)), \qquad (12a)$$

where $p_0$ is a normalization constant and the stochastic potential $\Psi$ is

$$\Psi(V) \equiv \int^V \frac{2U'(v)}{B_N^2(v)}\, dv + \ln(B_N)$$

$$= \frac{1}{M^2}\left\{\frac{3V^2}{8} + \frac{1}{2d}\left[\frac{V\text{sh}(4y)}{8} - \frac{5\text{ch}(4y)}{32}\right.\right.$$

$$\left.\left. + V\text{sh}(2y) - \text{ch}(2y)\right]\right\} + \ln(B_N), \qquad (12b)$$

where $y = dV + b$ for the special case of an additive noise (10), the PDF can be derived similar as in (12a) but with the stochastic potential proportional to the equilibrium potential $U$ as

$$\Psi(V) = \frac{2U(V)}{B_{0N}^2} \qquad (13)$$

In which $B_{0N} = B_0 M$.

Figures 5a and 5b show PDFs for the monostable system $d = 0.8$ in the reduced models of multiplicative (12) and additive (13) noises, respectively, while Figs. 5c and 5d show the corresponding PDFs for the bistable system $d = 1.2$. The reduced model of additive noise is simple: the PDF has the same modality as the equilibrium potential, which exhibits a single peak at $V = 0$ for
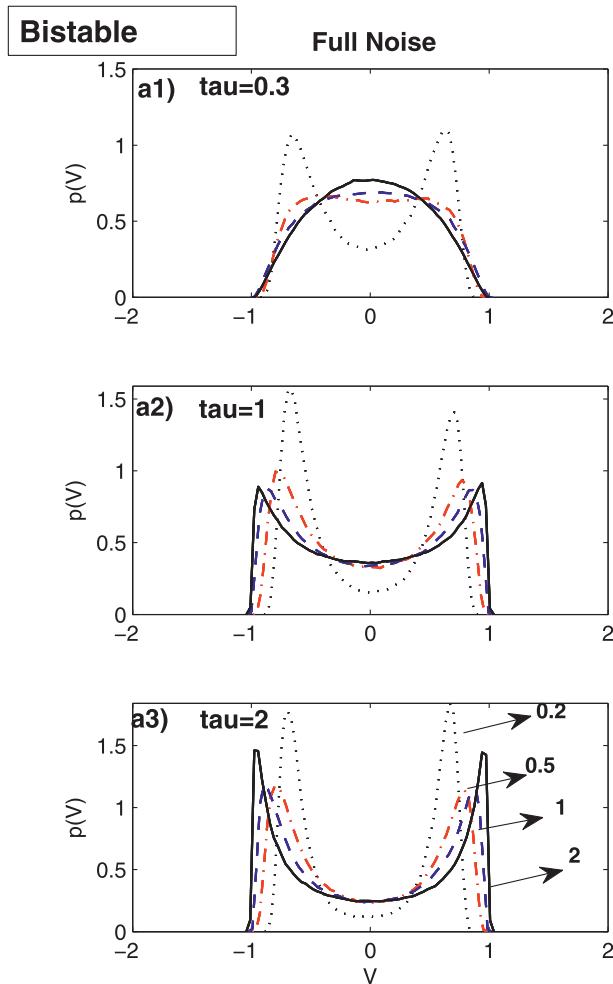
FIG. 4. Stationary PDF for the bistable system $d = 1.2$ in the full model with soil memories (top) $\tau = 0.3$, (middle) $\tau = 1$, and (bottom) $\tau = 2$. In each panel, four rainfall intensities are used: $\sigma = 0.2$ (dot), $\sigma = 0.5$ (dash–dot), $\sigma = 1$ (dash), and $\sigma = 2$ (solid), as marked in [a(3)].

the monostable system (Fig. 5b) but double peaks at $V \sim \pm 0.8$ for the bistable system (Fig. 5d). In both systems, the peak of the PDF spreads when the random forcing intensifies, reflecting the mixing effect on the PDF induced by the white noise forcing as shown in the last term of the Fokker–Planck Eq. (11).

In the reduced model of multiplicative noise, an increased noise induces two new modes (PDF peaks) at green and desert states in the monostable system while the old mode $V = 0$ is suppressed (Fig. 5a). This is easy to understand in Eq. (9): the multiplicative factor $B(V)$ is maximum at $V = 0$ and diminishes for a large magnitude of $|V|$. The strong noise forcing near $V = 0$ "pushes" the system away from the equilibrium state $V = 0$ such that this state no longer supports a PDF peak. In the meantime, once pushed far away from $V = 0$ on either side,

vegetation tends to stay there because there is little noise forcing, generating a new PDF peak.[2] This effect of multiplicative noise contributes critically to the bimodality in the full model, as will be discussed later.

The effect of colored noise on the reduced system is further examined numerically for the case of multiplicative-colored noise in (9) and (6) and additive-colored noise in (10) and (6). With the colored noise, there is no longer a general analytical solution to the PDF (Jung and Hänggi 1987; Monahan et al. 2002). Therefore, we will use numerical integration, as for the full model. The PDFs for the reduced models of multiplicative-colored and additive-colored noises are shown in Figs. 2b and 2c, respectively, for the monostable system $d = 0.8$, as in the full model in Fig. 2a. For both reduced models, one striking difference from the full model is the insensitivity of PDF to soil memory. Indeed, for different soil memories, the PDFs for the multiplicative-colored noise are similar to that of white noise in the analytical solution (Fig. 5a), changing from unimodal at weak forcing to bimodal at strong forcing; the PDFs for the additive-colored noise are also similar to that under white noise forcing in the analytical solution (Fig. 5b), with a single peak at $V = 0$.[3] This suggests that the effect of colored noise alone is insufficient for the generation of bimodality.

The PDF of the full model appears to resemble that of additive noise for short soil memory, being unimodal regardless of the forcing magnitude [Fig. 2a(1) versus Fig. 2c(1)], but it resembles that of multiplicative noise for slow soil memory, developing from unimodal to bimodal with the magnitude of the forcing [from Figs. 2a(2),(3) to Figs. 2b(2),(3)]. This can be understood as follows. In the full vegetation equation (1), the effect of diminishing $B(V)$ at large $|V|$ in the reduced model of multiplicative noise can be traced to the nearly constant equilibrium vegetation response $\tanh R$ near the green and desert states $V \sim \pm 1$ for large rainfall anomaly $|R| > |R_C|$ (Fig. 1a). Physically, if the vegetation is near the green state, it tends to stay there because precipitation is already more than sufficient such that a rainfall anomaly would have little impact on the vegetation. (A similar argument can be made on the desert state). In contrast, the vegetation is unlikely to stay near its equilibrium state $V = 0$, where it is easily "pushed" around by the noise. Effectively, then, vegetation tends to form two

---

[2] This effect of multiplicative noise in generating bimodality can be seen somewhat similar to that in a climate–soil model (Rodriguez-Iturbe et al. 1991).

[3] Similarly in the bistable case $d = 1.2$. For different soil memory, the PDFs remain similar to those under a white noise forcing (Figs. 5c,d) for both the multiplicative noise and additive noise (not shown).
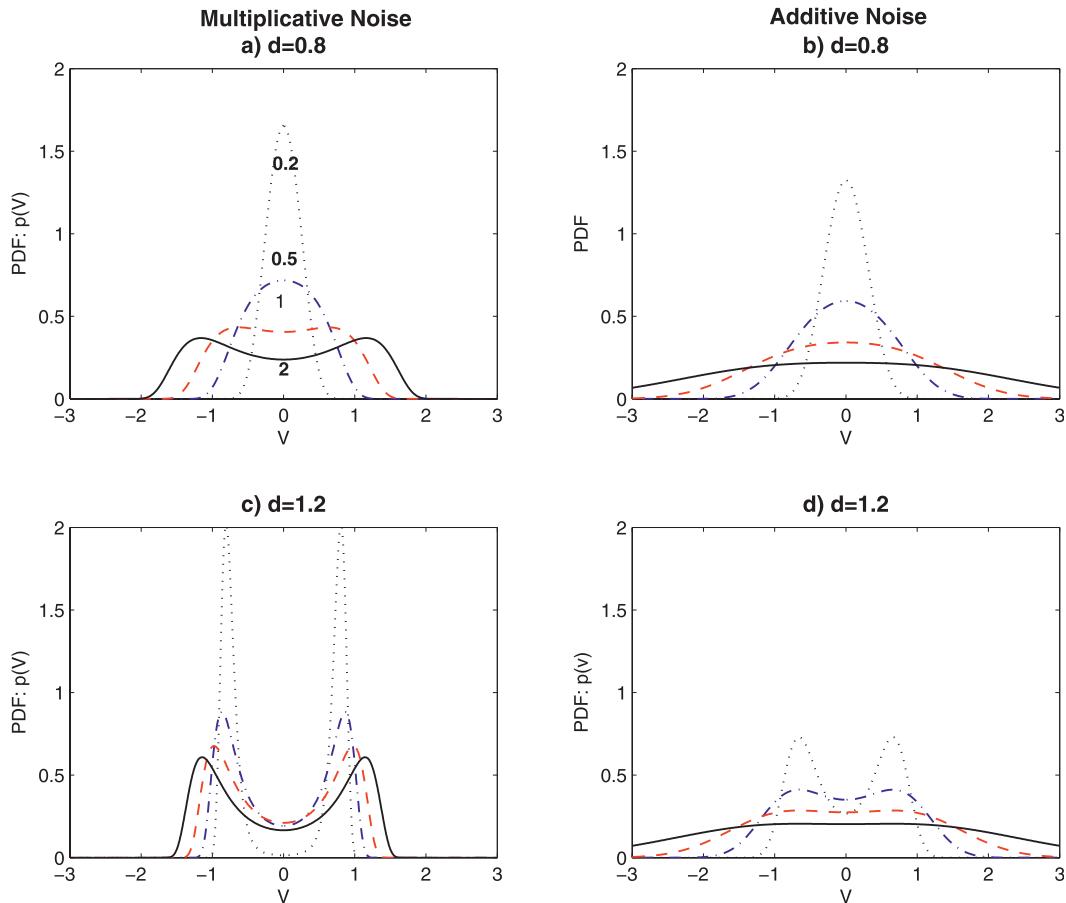
FIG. 5. Analytical solution of the stationary PDF forced by a white noise in the reduced models of (left) multiplicative and (right) additive noises: (a),(b) monostable ($d = 0.8$) and (c),(d) bistable ($d = 1.2$). In each panel, PDFs forced by four moisture variability intensities are plotted $\Sigma = 0.2$ (dot), 0.5 (dash–dot), 1 (dash), and 2 (solid), as marked in (a).

preferred states in the green and desert states in the full model, even if the system is monostable in its equilibrium at the medium state. Furthermore, the slow soil memory, and in turn, the slow noise, enables the vegetation to follow the nonlinear equilibrium vegetation response [as in Eq. (1)], which enables the stochastic noise to force the vegetation in a nonlinear way, which is critical for bimodality. Otherwise, with a fast noise, vegetation will be forced to change rapidly with little chance of approaching the nonlinear equilibrium response. Then, the PDF will be diffused as in the case of a white noise. Thus, in the full system, it is the combined effect of soil moisture memory and nonlinear stochastic forcing on vegetation that generates the bimodality.

## 5. Summary and discussion

We have studied the modal response of the vegetation states to precipitation variability in a conceptual climate–ecosystem model. The vegetation is found to exhibit bi-

modality in a monostable climate–ecosystem when forced by strong rainfall variability in the presence of a slow soil moisture memory. A systematic analysis suggests that the bimodality is generated by a nonlinear vegetation response to climate forcing and the resulting nonlinear response to colored stochastic forcing. The nonlinear vegetation response is such that vegetation becomes insensitive to rainfall changes once it reaches the green or desert state, generating two preferred modes there. The long memory of soil moisture slows down the precipitation noise such that vegetation has sufficient time to adjust toward the nonlinear equilibrium vegetation response.

Overall, our study suggests an important role of stochastic forcing in the bimodality of the climate–ecosystem. With a weak forcing, bimodality is determined completely by the stability of the equilibrium system and corresponds exactly to the regime of bistability ($d > 1$). This correspondence between bimodality and bistability is changed significantly by a strong stochastic forcing. With a short memory, stochastic forcing suppresses bimodality into
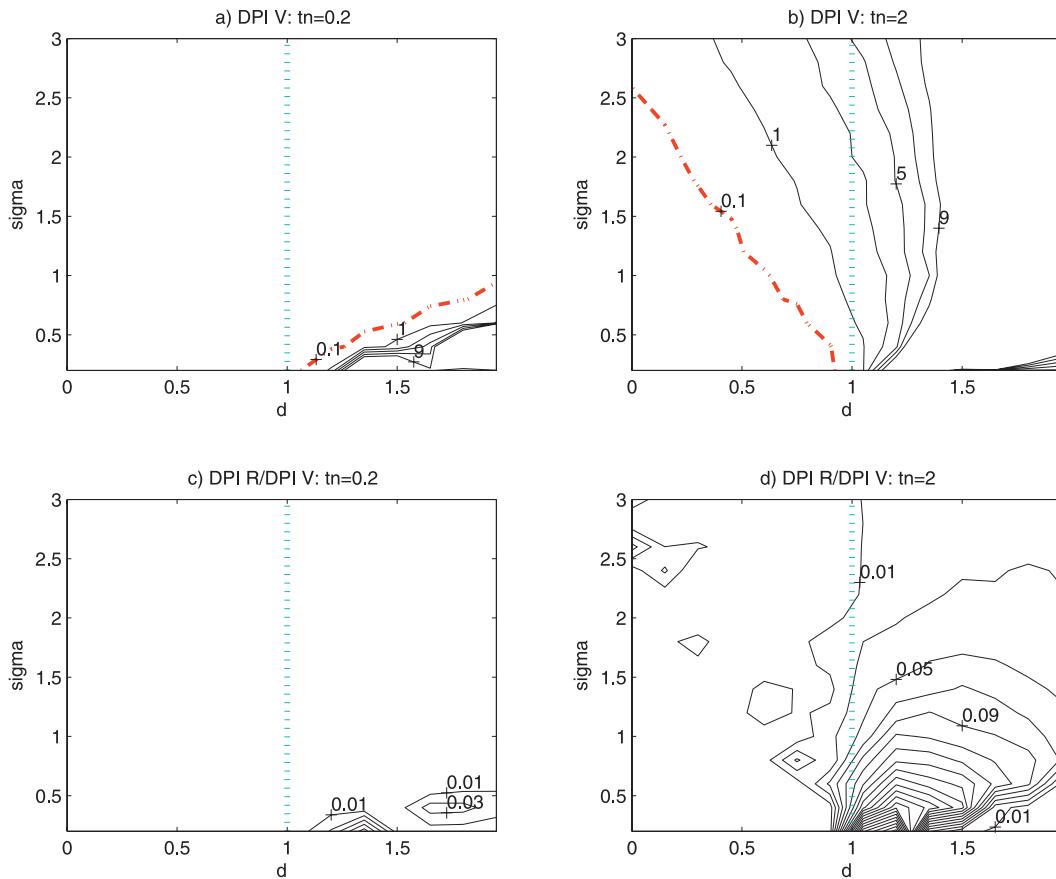
FIG. 6. Double-peak intensity for vegetation cover $V$ as a function of stability parameter $d$ and precipitation intensity $\sigma$ for (a) short ($\tau = 0.2$) and (b) long ($\tau = 2$) soil memory. Solid contours start from 1 to 9 with an interval of 2 (values above 9 are not shown). The dash–dot contour is for DPI = 0.1. The dot line $d = 1$ is the stationary boundary between monostable ($d < 1$) and bistable ($d > 1$) systems. (c),(d) Similar to (a) and (b), but for the ratio of double-peak intensity between total soil moisture ($R$) and vegetation cover ($V$) (for DPI of vegetation cover greater than 0.1). Contours start from 0.01 with an interval of 0.02. In (a),(b) the rainfall variability suppresses bimodality for short soil memory but enhances bimodality for long soil memory, respectively; in (c),(d) the bimodality is usually much weaker in the total soil moisture than in vegetation cover, especially in the monostable regime.

the bistable regime while, for a long memory, stochastic forcing expands bimodality into the monostable regime. This can be seen in the DPI as a function of the feedback parameter and the intensity of stochastic forcing in Fig. 6. For a short memory ($\tau = 0.2$, Fig. 6a), bimodality is suppressed almost completely across $d = 1$ deep into the unstable regime, except for the very unstable regime under a very weak forcing (the lower-right corner). In contrast, for a long memory ($\tau = 2$, Fig. 6b), significant bimodality emerges across $d = 1$ back deep into the monostable regime, especially for strong stochastic forcing on weakly stable systems. As a result, bimodality no longer corresponds to bistable regime. Instead, the boundary of bimodality is smeared across the boundary of stability ($d = 1$) with a short forcing suppressing bimodality and a long forcing favoring bimodality. Therefore, to understand the bimodality of the climate–

ecosystem, it is important to understand not only the stability of the equilibrium state, but also the characteristics of the noise forcing and its interaction with the coupled system.

It is also interesting to examine the bimodality of the total soil moisture $R$. This may have implications to the abrupt changes in the observation (LIU) and may also be relevant to the bimodality of soil moisture in the observation (D'Odorico and Porporato 2004). Since the soil moisture variability directly driven by precipitation variability $N$ is Gaussian, here Eq. (2) shows that the bimodality of $R$ can only be generated by the vegetation feedback $dV$. Therefore, the bimodality in $R$ should increase with the feedback parameter $d$. It is, however, unclear how much the bimodality of $R$ varies relative to that of $V$. Figures 6c and 6d show the ratio of the DPI of $R$ with the DPI of $V$ for the cases of a short and long soil

memory. For a short soil memory, there is virtually no bimodality in $R$ because the DPI of $R$ is two orders smaller than that of $V$ (Fig. 6c),[4] the latter being very small itself (Fig. 6a) because of the suppression of bimodality by fast rainfall variability. For a long soil memory, the bimodality in $R$ increases significantly with the instability parameter $d$ (Fig. 6d), suggesting a rapid increase of the bimodality of $R$ relative to that of $V$. In the monostable regime, the bimodality is very weak in $R$ because the DPI of $R$ is two orders smaller than that for $V$. Across the stability boundary into the unstable regime ($d > 1$), the DPI for $R$ increases much faster than that for $V$, by over 10 times, from a DPI ratio of 0.01 at $d = 1$ to larger than 0.1 for $d$ about 1.1 to 1.5 if the rainfall variability $\sigma$ is not too strong. It is interesting that a further increase of instability $d$ beyond ~1.5 leads to a decrease of the DPI ratio, which may be caused by a too fast increase of DPI of $V$ (Fig. 6b) there. Finally, as the noise intensifies, the bimodality of $R$ is always decreased relative to that of $V$ because of the increased contribution from the Gaussian $N$.

Our study may have important implications regarding the understanding of abrupt climate changes. In addition to the classical mechanism of positive feedback and multiple equilibria, our result suggests that abrupt changes of the ecosystem can also be induced by stochastic climate variability if the stochastic forcing is sufficiently slow and strong and acts nonlinearly on the coupled system. Therefore, to understand abrupt changes, we should study not only the stability the mean state but also the characteristics of the noise and its interaction with the nonlinear system. As for a coupled climate–ecosystem, our study provides a theoretical support for the proposal of LIU: the ecosystem can collapse abruptly in a monostable coupled climate–ecosystem in the presence of strong rainfall variability and slow soil memory. Furthermore, in contrast to a bistable system for which abrupt changes occur in both climate variables (such as precipitation, soil moisture) and ecological variables (such as vegetation cover), the abrupt change in a monostable system is shown most clearly in the ecological variable, rather than climate variables. Therefore, the relative magnitude of abrupt transition between the climate and ecosystem variables may provide a useful index to judge the nature of the abrupt change in a coupled climate–ecosystem.

## REFERENCES

Brovkin, V., M. Claussen, V. Petoukhov, and A. Ganopolski, 1998: On the stability of the atmosphere-vegetation system in the Sahara/Sahel region. *J. Geophys. Res.,* **103** (D24), 31 613–31 624.

Cessi, P., 1994: A simple box model of stochastically forced thermohaline flow. *J. Phys. Oceanogr.,* **24,** 1911–1920.

Claussen, M., 1998: On multiple solutions of the atmosphere-vegetation system in present-day climate. *Global Change Biol.,* **4,** 549–559.

——, C. Kubatzki, V. Brovkin, A. Ganopolski, P. Hoelzmann, and H.-J. Pachur, 1999: Simulation of an abrupt change in Saharan vegetation in the mid-Holocene. *Geophys. Res. Lett.,* **26,** 2037–2040.

deMenocal, P., J. Ortiz, T. Guilderson, J. Adkins, M. Sarnthein, L. Baker, and M. Yarusinsky, 2000: Abrupt onset and termination of the African Humid Period: Rapid climate responses to gradual insolation forcing. *Quat. Sci. Rev.,* **19,** 347–361.

D'Odorico, P., and A. Porporato, 2004: Preferential states in soil moisture and climate dynamics. *Proc. Natl. Acad. Sci. USA,* **101,** 8848–8851.

Gardiner, C. W., 1997: *Handbook of Stochastic Methods for Physics, Chemistry and the Natural Sciences.* Springer, 442 pp.

Hänggi, P., P. Talkner, and M. Brokovec, 1990: Reaction-rate theory: Fifty years after Kramers. *Rev. Mod. Phys.,* **62,** 251–342.

Jung, P., and P. Hänggi, 1987: Dynamical systems: A unified colored-noise approximation. *Phys. Rev.,* **A35,** 4464–4466.

Kloeden, P. E., and E. Platen, 1992: *Numerical Solution of Stochastic Differential Equations.* Springer, 632 pp.

Liu, Z., Y. Wang, R. Gallimore, M. Notaro, and C. I. Prentice, 2006: On the cause of abrupt vegetation collapse in North Africa during the Holocene: Climate variability vs. vegetation feedback. *Geophys. Res. Lett.,* **33,** L22709, doi:10.1029/2006GL028062.

Monahan, A. H., A. Timmermann, and G. Lohmann, 2002: Comments on "Noise-induced transition in a simplified model of the thermohaline circulation." *J. Phys. Oceanogr.,* **32,** 1112–1116.

Rodriguez-Iturbe, I., D. Entekhabi, and R. L. Bras, 1991: Nonlinear dynamics of soil moisture at climate scales 1. Stochastic analysis. *Water Resour. Res.,* **27,** 1899–1906.

Stommel, H., and W. R. Young, 1993: The average *T–S* relation of a stochastically forced box model. *J. Phys. Oceanogr.,* **23,** 151–158.

Timmermann, A., and G. Lohmann, 2000: Noise-induced transitions in a simplified model of the thermohaline circulation. *J. Phys. Oceanogr.,* **30,** 1891–1900.

Zeng, X., X. Zeng, S. S. P. Shen, R. E. Dickinson, and Q.-C. Zeng, 2005: Vegetation-soil water interaction within a dynamic ecosystem model of grassland in semi-arid areas. *Tellus,* **57B,** 189–202.

---

[4] The ratio of the DPIs between $R$ and $V$ depends on time scale of average. A time average should reduce the contribution of $N$ relative to that of $V$ if $N$ is faster than $V$ and, in turn, increase the DPI for $R$ and, in turn, the ratio. Therefore, in the discussion of the ratio of DPIs here, we should focus more on its relative changes with other parameters than its absolute value.